BBA - Molecular Basis of Disease 1864 (2018) 640–648

Contents lists available at ScienceDirect

BBA - Molecular Basis of Disease

journal homepage: www.elsevier.com/locate/bbadis

New perspectives for pharmacological chaperoning treatment in methylmalonic aciduria *cblB* type

S. Brasil[a,1], A. Briso-Montiano[a,1], A. Gámez[a], J. Underhaug[b], M.I. Flydal[c], L. Desviat[a], B. Merinero[a], M. Ugarte[a], A. Martinez[c,d,*], B. Pérez[a,**]

[a] Centro de Diagnóstico de Enfermedades Moleculares, Centro de Biología Molecular-SO UAM-CSIC, Universidad Autónoma de Madrid, Campus de Cantoblanco, 28049 Madrid/Centro de Investigación Biomédica en Red de Enfermedades Raras (CIBERER), Instituto de Investigación Sanitaria IdiPAZ, Madrid, Spain
[b] Department of Chemistry, University of Bergen, Norway
[c] Department of Biomedicine, University of Bergen, Norway
[d] KG Jebsen Center for Neuropsychiatric Disorders, University of Bergen, Norway.

ARTICLE INFO

Keywords:
Pharmacological chaperones
MMA *cblB* type
ATR
MMAB
Destabilizing mutations

ABSTRACT

Methylmalonic aciduria *cblB* type (MMA *cblB*) is caused by the impairment of ATP:cob(I)alamin adenosyltransferase (ATR), the enzyme responsible for the synthesis of adenosylcobalamin (AdoCbl) from cob(I)alamin. No definitive treatment is available for patients with this condition and novel therapeutic strategies are therefore much needed. Recently, we described a proof-of-concept regarding the use of pharmacological chaperones as a treatment. This work describes the effect of two potential pharmacological chaperones - compound V (N-{[(4-chlorophenyl)carbamothioyl]amino}-2-phenylacetamide) and compound VI (4-(4-(4-fluorophenyl)-5-methyl-1H-pyrazol-3-yl)benzene-1,3-diol) - on six ATR mutants, including the most common, p.Arg186Trp. Comprehensive functional analysis identified destabilizing (p.Arg186Gln, p.Arg190Cys, p.Arg190His, p.Arg191Gln and p.Glu193Lys) and oligomerization (p.Arg186Trp and p.Arg191Gln) mutations. In a cellular model overexpressing the destabilizing/oligomerization mutations, compounds V and VI had a positive effect on the stability and activity of all ATR variants. When provided in combination with hydroxocobalamin a more positive effect was obtained than with the compounds alone, even in mutations previously described as B_{12} non-responsive. In addition, a normal oligomerization profile was recovered after treatment of the p.Arg186Trp mutant with both compounds. These promising results confirm MMA *cblB* type as a conformational disorder and hence, pharmacological chaperones as a new therapeutic option alone or in combination with hydroxocobalamin for many patients with MMA *cblB*.

1. Introduction

Methylmalonic aciduria *cblB* type (MMA *cblB*, MIM *251110) is caused by the impairment of the mitochondrial enzyme ATP:cob(I) alamin adenosyltransferase (ATR, EC 2.5.1.17). ATR is a homotrimeric protein that catalyses the synthesis of adenosylcobalamin (AdoCbl) from cobalamin (vitamin B_{12}) using ATP to provide the adenosyl group. The AdoCbl produced acts as a cofactor for the mitochondrial enzyme methylmalonyl-CoA mutase (MUT, EC 5.4.99.2). MUT is responsible for turning L-methylmalonyl-CoA into succinyl-CoA, which then enters the tricarboxylic acid cycle [1]. ATR is encoded by the *MMAB* gene (MIM *607568) which consists of nine exons encoding a 250 residue protein that becomes fully functional after adopting a homotrimeric form [2–4]. Affected patients may present with either severe, early-onset disease characterized by neonatal ketoacidosis, lethargy, failure to thrive and encephalopathy, or milder late-onset disease in which the risk of severe complications including neurological impairment seems reduced or delayed over time. Treatment consists of dietary restriction based on low protein intake, and hydroxocobalamin (OHCbl), N-carbamylglutamate and carnitine supplementation, and also antibiotics to reduce propionate production by gut bacteria. None of these treatments, however, is definitive; indeed, only about 40% of patients

Abbreviations: AdoCbl, adenosylcobalamin; ATR, ATP:cob(I)alamin adenosyltransferase; DSF, differential scanning fluorimetry; HGMD, Human Gene Mutation Database; HTS, high-throughput screening; iPSCs, induced pluripotent stem cells; MMA, methylmalonic aciduria; MUT, methylmalonyl-CoA mutase; OHCbl, hydroxocobalamin; PAINS, pan assay interference compounds; PCs, pharmacological chaperones; PR, proteostasis regulators; SMARTS, Smiles Arbitrary Target Specifications

* Corresponding author.
** Correspondence to: B. Pérez, Centro de Diagnóstico de Enfermedades Moleculares, Centro de Biología Molecular UAM-CSIC, Universidad Autónoma Madrid, Madrid, Spain.
E-mail addresses: Aurora.Martinez@uib.no (A. Martinez), bperez@cbm.csic.es (B. Pérez).
[1] These authors contributed equally to this work.

https://doi.org/10.1016/j.bbadis.2017.11.024
Received 3 August 2017; Received in revised form 17 November 2017; Accepted 27 November 2017
Available online 02 December 2017
0925-4439/

respond to OHCbl [5]. In recent years, liver or liver/kidney transplantation has also become an option [6], although such procedures are not without danger and entail severe problems, such as the need for immunosuppression.

We have previously described and characterized destabilizing mutants of ATR in which some residual activity is retained, as well as a number of possible pharmacological chaperones (PCs), one of which is able to rescue p.Ile96Thr [7,8]. Since more than 50% of the reported mutations in *MMAB* are missense mutations (HGMD® Professional 2016.3), which most often lead to unstable, misfolded proteins, PCs and/or proteostasis regulators (PRs) could represent treatment options for many patients.

PRs are small compounds that increase proteostasis capacity by activating the quality control system (QCS), involving both molecular chaperones that stimulate proper folding and protein degrading systems such as ubiquitin (Ub)-dependent proteasome and Ub-independent degradation [9,10]. PCs are small protein-specific molecules that stabilize the native state and/or modify mutant protein structure, shifting the equilibrium toward the folded state [11]. PCs can be active-site binders, which are often inhibitory, or they may bind at other sites in their target enzyme, such as allosteric sites [12,13]. Although it has been postulated that specific inhibitors render better results than non-specific stabilizers [11], the next generation of PCs under development for different conditions is based on non-inhibitory compounds [14–16]. Furthermore, a positive, synergistic effect of the combination of PRs and PCs has been demonstrated [17,18] in the treatment of severe disease phenotypes.

This work reports the impact of known mutations at residues Arg186, Arg190, Arg191 and Glu193, located in a region important for the enzymatic function, and the effect of compounds V and VI [8] alone or in combination with OHCbl. Both prokaryotic and eukaryotic models expressing the pathogenic variants p.Arg186Gln, p.Arg186Trp, p.Arg190Cys, p.Arg190His, p.Arg191Gln and p.Glu193Lys [19] were used to evaluate the possibility of extending the use of therapeutic PCs to patients with these mutations.

2. Results

2.1. Characterization of the selected ATR mutations

Six mutations were examined to determine whether they were destabilizing, and thus candidates for rescue by PCs. These included the most common pathogenic mutation p.Arg186Trp which occurs in over 30% of the reported alleles, as well as others detected in patients around the world: p.Arg186Gln, p.Arg190Cys, p.Arg190His, p.Arg191Gln and p.Glu193Lys [19,20] (Fig. S1). All mutations are located in invariant residues in close proximity that are fundamental for proper protein function [2].

The effect of these mutations on the oligomerization, stability and activity of ATR was examined. Human His_6-ATR wild-type (WT) and p.Arg186Gln, p.Arg186Trp, p.Arg190Cys, p.Arg190His, p.Arg191Gln and p.Glu193Lys mutant proteins were expressed in a prokaryotic system. The amount of protein obtained was analysed by western blotting. Bacteria expressing the WT and mutant proteins were grown at 37 °C. The corresponding protein fractions were obtained, and equal amounts of total protein loaded onto an SDS-PAGE gel. Fig. 1A shows that all the mutant ATR proteins, except p.Arg191Gln are produced in similar amounts to WT.

Following protein expression and affinity purification, the oligomerization profiles of the ATR variants were analysed by size-exclusion chromatography (Table 1, Fig.1B). The p.Arg186Gln, p.Arg190Cys, p.Arg190His and p.Glu193Lys mutations produced oligomerization profiles similar to that of WT, with large amounts of trimeric protein and low proportions of aggregates and monomers. The p.Arg186Trp mutation was associated with a reduction in trimer formation (31.6% compared to 91.2% for WT) and an increase in monomers of about 65%

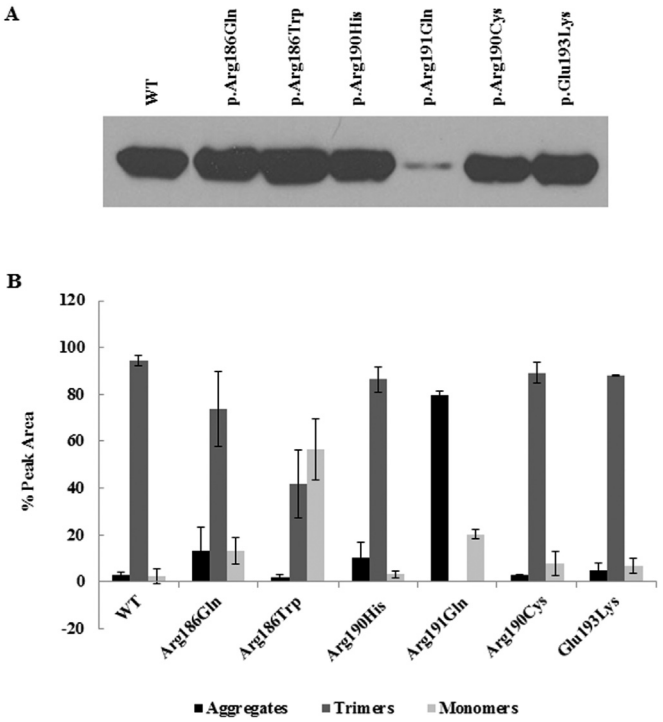

Fig. 1. Expression and oligomerization profile of WT and mutant ATR. A: Western blots of WT and ATR mutants. Equal amounts (10 μg) of recombinant protein, obtained using the prokaryotic expression system, were loaded onto an SDS-PAGE gel. B: Percentage of aggregates, trimers and monomers for WT and ATR mutants. The total amount of purified protein was considered to represent 100% in each case.

compared to the WT. The p.Arg191Gln mutant produced no trimeric form of the protein and its oligomerization profile showed only aggregates (81%) and monomers (19%) (Fig.1B).

The thermal stability of the WT and mutant ATRs was then analysed by differential scanning fluorimetry (DSF) using the trimeric form of the purified proteins (Table 1). All variants, except p.Arg186Trp, showed a melting temperature (T_m) downshift of 3.0–6.7 °C with respect to WT, indicating their intrinsic instability. The stability of p.Arg186Gln was least affected, with a 3 °C downshift from WT T_m, while the Tm of mutant p.Glu193Lys was lowered by 6.7 °C and was thus the most destabilized mutant. The p.Arg186Trp mutant showed a 2.5 °C-increase in T_m compared to the WT and the p.Arg191Gln mutation could not be analysed since no trimeric protein could be obtained.

The effect of these mutations on ATR activity was analysed using a cellular model of the disease. Patient-derived fibroblasts bearing the null mutations c.290G > A and c.349-1G > C [7], which produce neither immunoreactive ATR protein nor detectable ATR enzymatic activity, were transduced with a lentivirus expressing the WT or mutant ATRs, and enzymatic activity was measured with a coupled assay [21]. Initially, all the mutants showed diminished enzymatic activity when compared with WT ATR. p.Arg186Trp showed the greatest residual activity, (90%), while p.Glu193Lys showed the lowest amount with 20% of residual activity when compared with WT. The three other mutant proteins presented between 50 and 70% of residual activity. It is noteworthy that residual activity is increased by overexpression of the destabilizing mutations.

2.2. Binding affinity and molecular docking

The affinity of compound VI for WT ATR was measured by the concentration-dependent thermal stabilization of the enzyme using DSF. Purified trimeric ATR was titrated with compound VI (0–100 μM) (Fig. 2A), and the effect of the ligand on the T_m of ATR was analysed as described [22]. A K_d-value of 2.2 ± 0.2 μM was calculated, revealing a

Table 1
Characterization of the effect of the mutations on the stability and conformation of recombinant ATR mutants.

Mutation		DSF	Oligomerization Profile (% of peak area mAu*min[a])			Protein amount	Structural analysis (Function)	Mutant type
Protein	cDNA	T_m (°C)	Aggregates	Trimers	Monomers			
WT		61.4 ± 0.3	8.8	91.2	2.4			
p.Arg186Gln	c.557G > A	58.4 ± 1.3***	5.8	85.1	9.2	Normal	Generation of AdoCbl	Destabilizing
p.Arg186Trp	c.556C > T	64.0 ± 1.8***	2.8	31.6	65.7	Normal	Generation of AdoCbl	Oligomerization
p.Arg190Cys	c.568C > T	56.7 ± 1.4***	3.0	89.1	7.9	Normal	MgATP binding	Destabilizing
p.Arg190His	c.569G > A	56.8 ± 0.8***	5.5	90.3	4.2	Normal	MgATP binding	Destabilizing
p.Arg191Gln	c.572G > A	ND	81.0	NO	19.0	Reduced	Trimer interface	Destabilizing/ Oligomerization
p.Glu193Lys	c.577G > A	54.7 ± 1.0***	5.0	88.1	6.9	Normal	MgATP binding	Destabilizing

[a] SD is shown in Fig. 1B .
NO Not observed.
*** $P < 0.001$.

large affinity for a primary hit. The K_d-value for the binding of compound V has earlier been calculated to be 7.4 ± 0.4 μM [8]. Chemical structures of compound V and VI are depicted in Fig. S2.

Molecular docking for compound V has previously identified the most probable binding site for this compound, located at the C-terminal end of each subunit in the trimeric ATR (residues 228–240), and the loop 165–175, adjacent to the binding site of cobalamin [8]. For compound VI, the top-score cluster is located on the opposite side of the protein, where compound VI binds in the trimer interface, maintaining interface stability and proper oligomerization (Fig. 2B–D). This pocket is solvent accessible and in the best-ranked pose the compound establishes potential hydrogen bonds to the side chains of Asp79, Asp80, and Gln81. The matching and complementary steric and polar interactions of compound VI with trimeric ATR largely explain the high affinity of this hit compound.

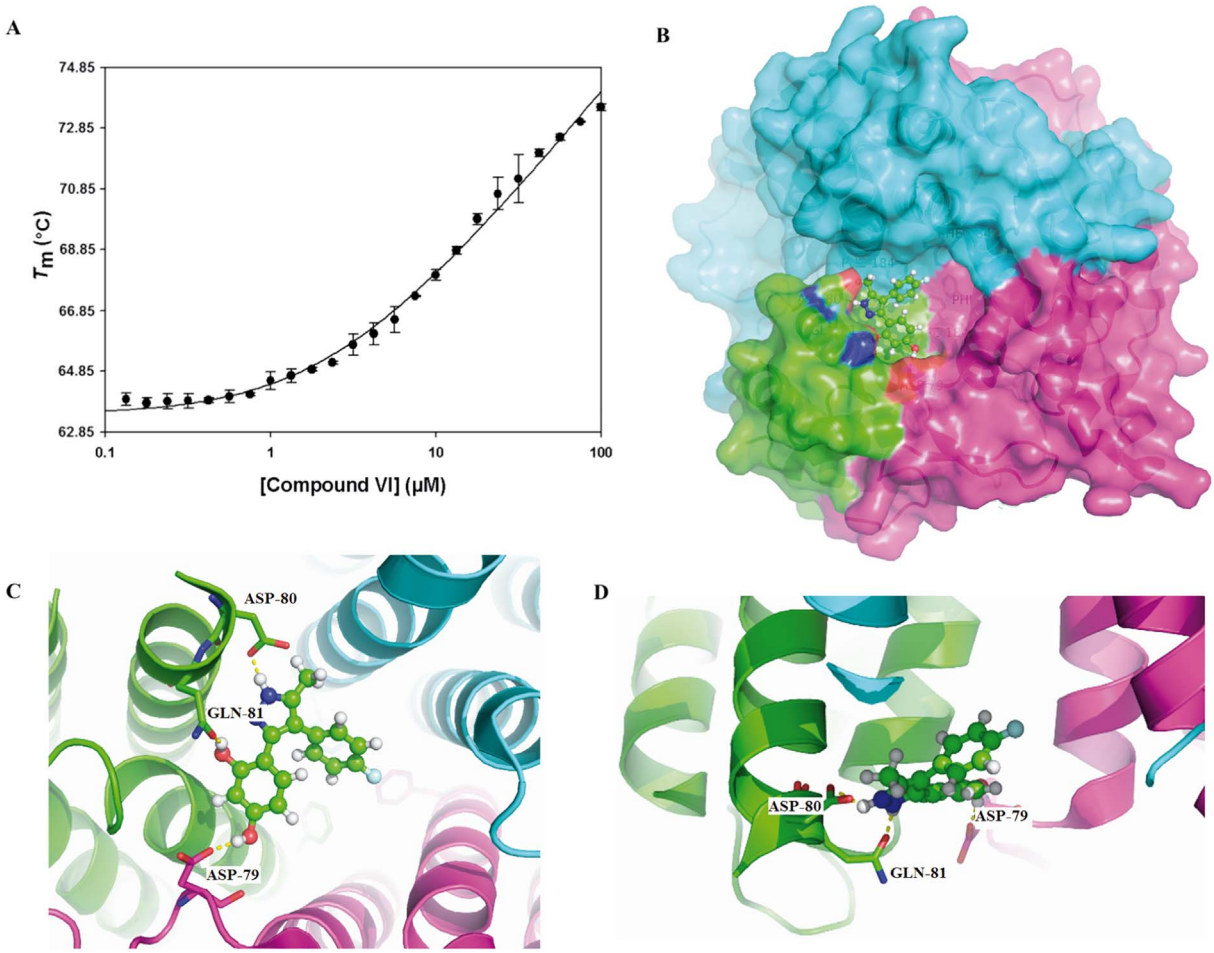

Fig. 2. The high affinity binding of compound VI to ATR. A: Effect of increasing concentration of compounds VI on the thermal stability of trimeric ATR as measured by DSF. A K_d value of 2.2 ± 0.2 μM was estimated according to the algorithm by Cooper and MacAuley-Hecht [22]. B: Overview of ATR (PDB ID 2IDX) showing the location of the proposed binding site for compound VI, in the base of the trimeric helical arrangement, as obtained from molecular docking. The top score pose from SwissDock is shown. Each subunit is presented in a different colour. (C and D) Detailed view of the proposed binding site for compound VI (ball-and-stick). The residues Asp79, Asp80 and Gln81, with which compound VI interacts in the docked structure, are shown represented with sticks.

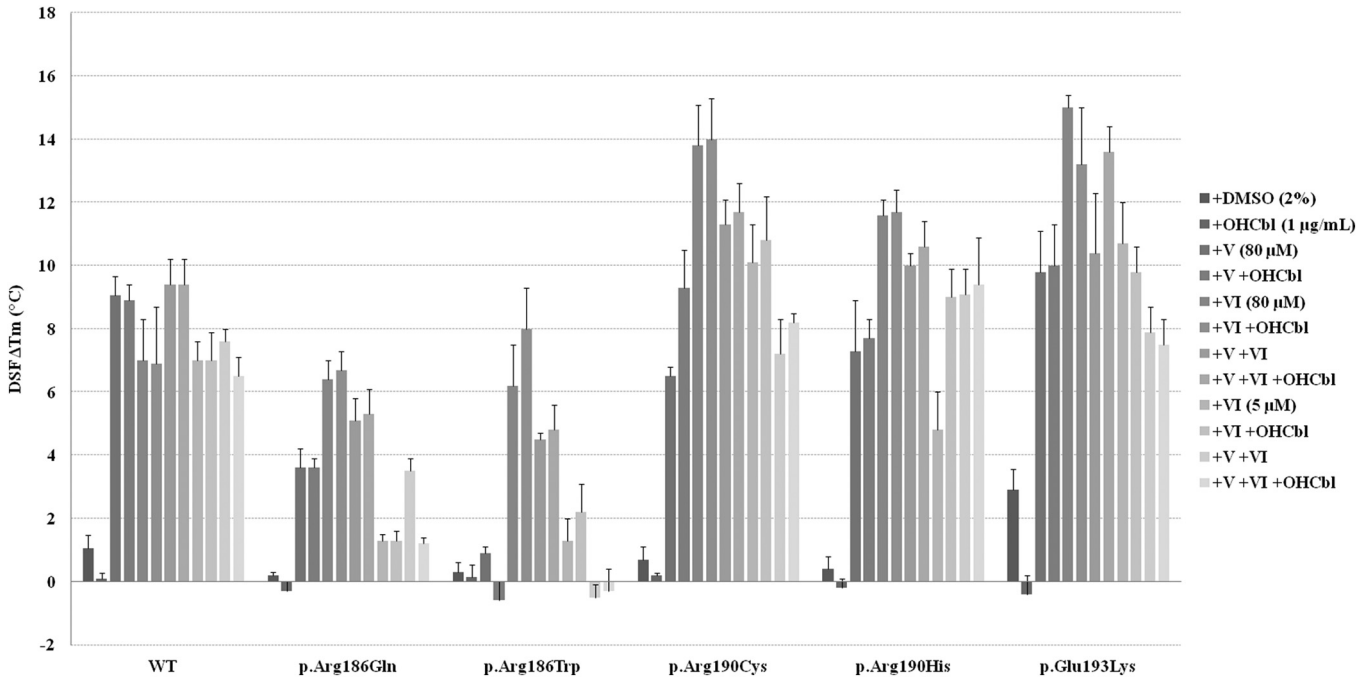

Fig. 3. Effect of compounds V, VI and OHCbl on the thermal stability of mutant and WT ATR proteins. Data (given as fold change in ΔT_m (°C) of each protein without any treatment as baseline) represents the mean ± SD of at least three independent experiments. ND – Not determined. $^{***}P < 0.001$.

2.3. Effect of two possible PCs on ATR mutant thermal stability, protein activity and oligomerization profile

The thermal stabilization of the mutant ATR proteins by compounds V and VI (Fig. S2), comparative to the WT, was performed by DSF (Fig. S3). No analyses could be performed for the p.Arg191Gln mutant since no purified recombinant protein could be obtained. As for WT the mutant ATR proteins displayed a concentration-dependent increase in thermal stability in the presence of one or the other PC, although to a less extent for p.Arg186Gln and p.Arg186Trp in the presence of compound V (Fig. S3). All mutants actually appeared responsive to 80 μM of either PC and this concentration was selected for cellular analyses. However, given its cytotoxicity in patient-derived fibroblasts (Fig. S4), compound VI was also tested at 5 μM. Specific ΔT_m-values ($T_m = T_m$-$T_{m,0}$, where $T_{m,0}$ is the T_m without compound) with compounds V or VI at 80 μM, compound VI at 5 μM, or OHCbl at 1 μg/mL are summarized in Fig. 3. Additionally, the effects of all these possible combinations were also analysed. OHCbl alone did not increase the thermal stability of any of the studied mutants, but both the PCs tested had a positive effect at the concentrations used, although to a less extent for mutants p.Arg186Gln and p.Arg186Trp. Compound VI was responsible for a higher stabilization in these two mutants compared to the same concentration of compound V, and although a stabilizing effect was also registered at a lower concentration (5 μM), this was less prominent. Therefore, compound VI appears to induce a more marked concentration-dependent effect on these two mutants.

Since p.Arg186Trp affects ATR oligomerization, the effect of compound V and VI on trimerization was tested. The p.Arg186Trp mutant was expressed in the presence of 80 μM of each compound and the oligomerization profile was examined. Before the treatment, the different oligomeric forms elute in a broad peak, with no distinct elution bands for the trimeric and monomeric forms of the protein, probably due to quick exchange between the different unstable forms. The percentage of monomers and trimers was estimated according to their expected elution time (Fig. 4A). However, after treatment with both compounds, two fractions became clearly separable (Fig. 4B); with the proportion of trimers increasing to approach WT levels (Fig. 4C).

To further evaluate the therapeutic potential of compounds V and VI on ATR activity, the cells over-expressing the ATR mutants were incubated for 72 h at 37 °C in the presence of 80 μM of compound V or 5 μM of compound VI in combination with 1 μg/mL of OHCbl, or OHCbl alone. The effect of the combination of all three compounds was also studied (triple combination). After 72 h of treatment, cells were collected for either immunoblotting or incubation with [^{14}C]-propionate to quantify the uptake of radiolabelled material, in an indirect, coupled assay of ATR activity (Fig. 5). All mutant proteins showed a significant increase in enzymatic activity after combining either compound with OHCbl, with the greatest increase observed for mutant p.Glu193Lys under all treatment combinations. Initially, this mutant showed the least residual activity. Mutant p.Arg191Gln showed the smallest increase in residual activity under all treatment combinations. Treatment with all combinations (especially the triple combination) produced an increase in ATR activity in all the mutants analysed, even reaching healthy derived-fibroblasts levels for p.Arg186Gln and p.Arg186Trp (data not shown).

2.4. Pharmaco-chemical analyses of the candidate PCs

The structures of compounds V and VI were chemically analysed using the SmartsFilter (Table 2) and Molinspiration bioinformatic tools (Tables S1 and S2). The first is a chemical filter that alerts to undesirable chemical features, while the second allows physicochemical properties to be determined. The SmartsFilter program (available online) uses Smiles Arbitrary Target Specification (SMARTS) queries, the same system used by pharmaceutical companies to identify substructures of interest. Although neither compound passed all filters, they do not belong to the pan assay interference compound (PAINS) category [23], whose members often show a broad and non-specific spectrum of biological activity [24]. Compound VI failed the ALARM NMR filter, suggesting it to be thiol-reactive [25], while compound V failed all the filters except for OPREA and PAINS, indicating it to have a more chemically challenging structure. The molecular properties and bioactivity scores for each compound were determined using the Molinspiration program (available online). Tables S1 and S2 show that both compounds have a number of atoms in the range of 20–70, < 10 rotatable bonds, and a polar surface area of < 140 Å^2, indicating drug-

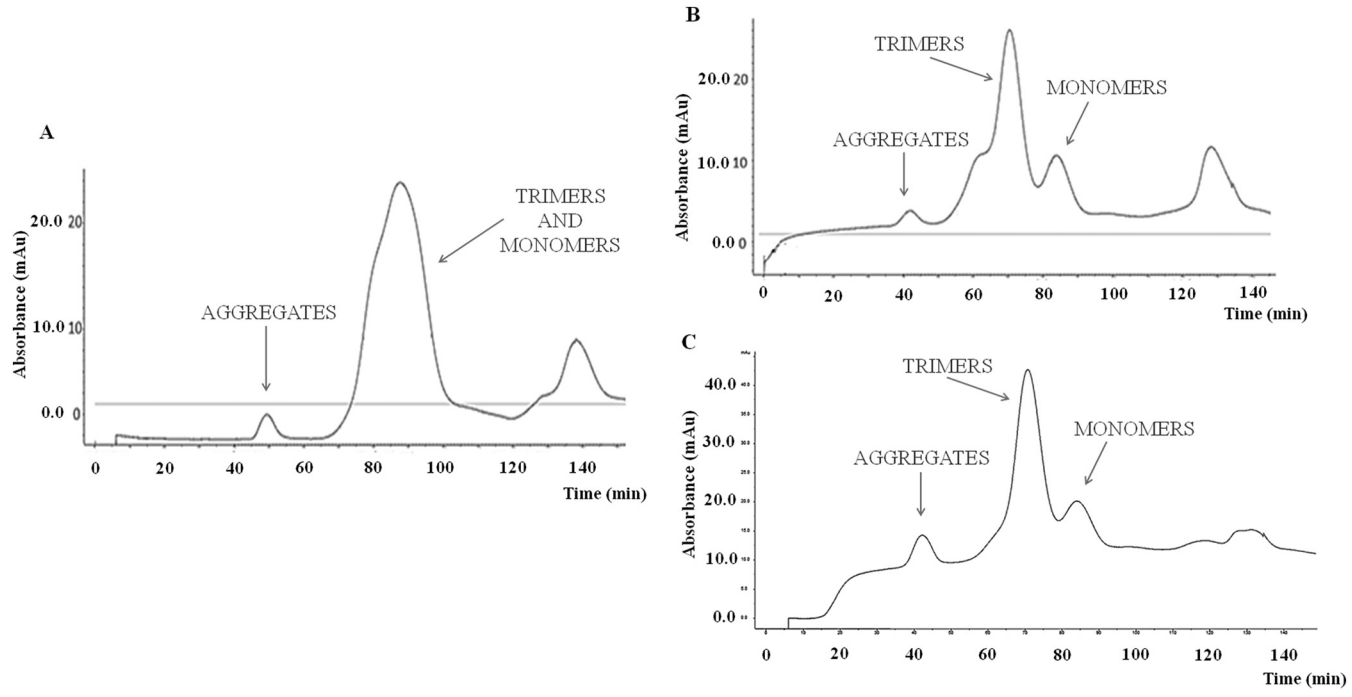

D

Mutation / Protein	Oligomerization Profile (% of peak area mAu*min)		
	Aggregates	Trimers	Monomers
WT	8.8	91.2	NO
p.Arg186Trp	2.8	31.6	65.7
p.Arg186Trp + VI	2.8	79.5	17.7
p.Arg186Trp + V	8.3	77.2	14.4

Fig. 4. Oligomerization profile of mutant p.Arg186Trp after treatment with compound VI. Using a prokaryotic system, p.Arg186Trp was expressed for 5 h in the presence of 80 μM of VI or compound V. After this, protein was purified and size-exclusion chromatography performed to show the oligomerization profile before (A) and after (B) incubation with either compound VI or (C) V. The percentage of aggregates, trimers and monomers was also calculated before (where the percentage of monomers and trimers was estimated by peak deconvolution according to the expected elution time for each form) and after incubation with both compounds (D). NO: not observed.

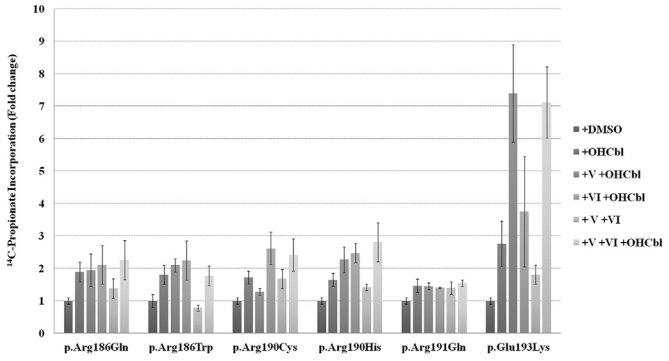

Fig. 5. Effect of the two possible PCs (V and VI) and OHCbl in a cellular disease model. Cells were incubated with 1 μg/mL OHCbl, 80 μM compound V, 5 μM compound VI or the equivalent volume of DMSO. After 72 h, ATR activity was measured in a coupled assay *via* [^{14}C]-propionate incorporation into acid-precipitable material in intact cells grown in basal medium. Data (as fold change regarding treatment with DMSO as 1) represents the mean ± SD of three independent experiments. $^{*}P < 0.05$, $^{**}P < 0.01$, $^{***}P < 0.001$.

like properties essential for good oral bioavailability [26,27]. The higher the bioactivity score, the more active a compound is. Scores above 0.0 describe compounds that are active, scores between −0.5 and 0.0 indicate moderate activity, and those below −0.5 reveal inactivity. Compound VI had an active profile for nuclear receptor ligand activity and kinase inhibitory activity, while compound V was negative for all properties tested.

3. Discussion

No definitive treatment exists for MMA *cblB* type. Although pharmacological doses of OHCbl can be administered, only about 40% of patients experience a positive biochemical response [5]. In the era of precision medicine, the challenge is to find orphan drugs for these patients [31], but in order to do so the molecular basis of the disorder must be established. Until now, several conformational disorders have been described, and one of the most promising therapies is based on the use of small drugs such as PCs and PRs [11] - an area of growing interest for pharmaceutical companies.

The present work assessed the selected pathogenic ATR mutations as potential candidates for rescue by folding therapies. Functional analysis allowed the identification of mutants showing defects mainly

Table 2
Analysis of the pharmaco-chemical properties of compounds V and VI using the SmartsFilter website.

	Smarts					
Compound	Blake[a]	Glaxo[b]	PAINS[c]	Oprea[d]	ALARM[e] NMR	Toxicity
Compound V (N-{[(4-chlorophenyl)carbamothioyl]amino}-2-phenylacetamide)	Positive	Positive	**Negative**	**Negative**	Positive	Positive
Compound VI (4-(4-(4-fluorophenyl)-5-methyl-1H-pyrazol-3-yl)benzene-1,3-diol)	**Negative**	**Negative**	**Negative**	**Negative**	Positive	**Negative**

[a] Blake: This set is from James Blake of Array Biopharma (published as contributed Sybyl script lint_sln.spl, formerly bundled with Sybyl) [28].
[b] Glaxo: The Glaxo set is comprised of an "unsuitable leads" subset, an "unsuitable natural products" subset, and a reactive subset. Optional Glaxo subsets are electrophilic and nucleophilic [29].
[c] PAINS "Pan-Assay Interference Compounds": Developed by Jonathan Baell and Georgina Holloway of The Walter and Eliza Hall Institute of Medical Research, Bundoora, Victoria, Australia [23].
[d] Oprea: Developed by Tudor Oprea, for general multi-objective library fitness [30].
[e] Alarm NMR: The ALARM NMR set derives from the published Abbott method and the supplemental materials from that paper [25].

in stability (p.Arg186Gln, p.Arg190Cys, p.Arg190His, p.Arg191Gln and p.Glu193Lys) or oligomerization (p.Arg186Trp and p.Arg191Gln), based on the amount of protein produced, the oligomerization profile and/or the activity of the ATR produced in a bacterial and a eukaryotic system. The trimeric form of all the mutant ATR proteins showed reduced thermal stability compared with WT, except for p.Arg186Trp, which showed increased thermal stability. In the native structure Arg186 is aligned with His183 and Arg190 on the same side of the α-helix, and these unfavourable electrostatic interactions are not properly compensated by acidic residues, explaining why the substitution by Trp may be favourable at the subunit level and thus explain the increase in conformational stability. On the other hand, Arg186 is located at the subunit interfaces in the trimer, and substitution by the bulkier Trp is expected to introduce both steric clashes and to perturb the compensatory surface electrostatic distribution in the trimeric structure. Although Arg186 had been implicated in OHCbl binding, the low affinity of p.Arg186Trp for AdoCbl indicates that residue Arg186 has a role in the transfer of the 5′-deoxyadenosyl group from ATP to the cofactor for the generation of AdoCbl [20]. Hence, p.Arg186Trp impairs the formation of AdoCbl despite the presence of OHCbl which might justify the lack of response of this mutation to pharmacological treatment with OHCbl. The adverse effect of this mutation appears to be reverted upon binding of both compounds V and VI. No recombinant trimeric protein could be obtained for p.Arg191Gln, suggesting that the mutation has a severely negative impact on protein stability and oligomerization. In fact, residue Arg191 is thought to be involved in the charged trimer interface [2], explaining the lack of trimeric ATR. Finally, all the ATR mutants showed reduced activity, ranging from 14% (p.Arg186Trp) to 80% (p.Glu193Lys) compared to WT. Residue Glu193 is important for the physiological coordination of Mg^{2+}, and its disruption might hinder ATP binding [2]. Since this is a crucial step for ATR activity, it could explain the drastic reduction in activity shown by this mutant. It should be noted that the residual activity in the cellular model was greater than that detected in the primary patient-derived fibroblasts. Similar results have been reported for the PMM2-CDG destabilizing mutations [32].

All mutants showed increased stability in the presence of compounds V or VI, or both - except for p.Arg186Trp, on which compound V exerted little stabilizing effect. None of the mutants showed an increase in thermal stability in the presence of 1 μg/mL OHCbl alone, but its combination with compound V, and especially compound VI, resulted in a significant increase in the stability of all mutants. Titration with both compounds (0–200 μM) showed a thermal stabilization for all mutants and WT-ATR, although to a less extent for p.Arg186Gln and p.Arg186Trp in the presence of compound V. These results highlight the potential effect of both compounds, and suggest that hit-to-lead optimization should be performed aiming at avoiding cellular off-targets.

All the ATR mutants showed an increase in activity upon treatment with OHCbl, indicating that although this compound alone did not increase their thermal stability using the recombinant protein it did exert a positive effect on these proteins *ex vivo*. This finding underscores the importance of subjecting candidate rescue compounds to multisystem assays. It is important to note that OHCbl needs to be enzymatically modified in the cellular environment, which explains the difference between the thermal denaturation and enzyme activity results. The positive response observed in the cellular system used does not correlate with the lack of response observed in patient-derived fibroblasts bearing some of the studied mutations [33], suggesting that the overexpression or possible protein rescue by pharmacological treatment of the mutant proteins allow the observed positive effect of cobalamin.

It is also important to note that treatment with each compound in combination with OHCbl, and the combination of both compounds with OHCbl, increased ATR enzymatic activity compared to the administration of OHCbl alone. For the p.Arg186Trp and p.Arg190Cys mutants, the greatest increase (more than double) was obtained after treatment with the combination of compound VI + OHCbl, while for mutants p.Arg186Gln, p.Arg190His, p.Arg191Gln and p.Glu193Lys, the combination of both compounds + OHCbl was the most effective. The p.Glu193Lys mutant showed an impressive recovery of enzyme activity compared to all other mutants, probably due to the fact that it showed the lowest activity in the absence of compounds.

The results reveal the particularly positive effect of compound VI; the recovery observed with a dose of just 5 μM is similar to the obtained for compound V at 16 fold that dose and confirms the higher affinity displayed by this compound toward ATR protein, when compared with compound V. Despite its toxicity in patient-derived fibroblasts, toxicity analyses in HepaRG™ cells (Fig. S5) demonstrate no toxic effects at higher concentrations for this compound, stressing the need to find good disease models for compound testing. Hence, after hit-to-lead optimization and off-target elimination, compound VI might prove to be the better option as a chaperone treatment for patients with loss-of-function mutations.

Combining compounds V and VI had no significantly enhanced effect on the majority of mutant proteins than the DMSO vehicle alone; this changed, however when they were further combined with OHCbl. Since compounds V and VI appear to bind at different binding sites, different to the active site (as predicted by molecular docking), no interference was expected. This implies either a role of OHCbl as an adjuvant for the positive effect of these compounds over ATR stability or a positive effect by the simultaneous binding of both compounds on cobalamin interaction. OHCbl co-administration with PCs could be a good strategy when dealing with mutants less responsive to compound V or VI alone, or when faced with non-responsive mutations. The combination of compounds, such as PCs and PRs, for the treatment of inherited metabolic disorders, and even the combination of different strategies, has been described for lysosomal storage disorders [34–36], cystic fibrosis [37], Niemann-Pick type C [38] and phenylketonuria [39,40], among others. The use of PRs might induce a protective environment for the mutant protein, and potentiate the corrective action of PCs, as described for other disorders [11].

Successful drug discovery requires candidate compounds to be effective not just *in vitro* or *ex vivo*, but *in vivo*, and this in turn depends on good (usually oral) bioavailability and pharmacokinetics [41]. In recent years, the number of 'academic drug discoveries' has increased, but the majority of compounds recorded as possible PCs have failed through being chemically unfit, falling for instance into the PAINS (Pan-Assay Interference Compounds) category class [42,43]. To ensure that compounds identified by high-throughput screening are good drug candidates, Lipinski's "rule of five" should be fulfilled [44,45]. A number of bioinformatics tools have also been developed to analyse the chemical structure of the compounds identified. Compound VI passed five of the six filters, but was flagged as ALRM NMR positive, a consequence of its thiol-reactive structure. Compound V was flagged by four of the six filters (Table 2). However, neither fell into the PAINS category. Both compounds have miLogP values of < 5, less than 10 rotatable bonds, and a topological polar surface area (TPSA) of < 140 $Å^2$ (Table S1), factors that indicate good oral bioavailability [26]. Since the brain is affected in MMA *cblB*, it is essential that these PCs can cross the blood brain barrier (BBB). Compounds with a TPSA of < 60–70 $Å^2$ tend to be CNS-active [27]. Also, if the number of nitrogen and oxygen atoms in a molecule is under five, it has a chance of crossing the BBB [45]. Both compounds share the latter characteristic, indicating that they could be CNS-active. Bioactivity scores also need to be known to establish the "druglikeness" of candidate compounds. The higher the score, the greater the probability of a compound being drug-like. Compound V returned very low scores, all under − 0.50, suggesting it to be different to any known drug (Table S2).

The advance in personalised medicine goes hand in hand with the evaluation of the potential drugs in appropriate disease models that can recapitulate disease pathophysiology. Although patient-derived fibroblasts are affordable and easy to obtain, they are not the best disease models and may influence test results as observed for the difference in compound VI toxicity. Nevertheless, animal models for testing mutation-specific therapies are somewhat difficult to obtain. Thus disease-relevant cell types, such as hepatocytes, derived from induced pluripotent stem cells can be an excellent disease model for preclinical studies [46].

In summary, this work confirms the potential of using conformation-stabilizing therapies in the treatment of patients with MMA *cblB*. The two non-mutations specific PCs described, which increased the effect of OHCbl, should be evaluated as hit-to-lead chemical compounds in other *ex vivo* cellular models with a view to their *in vivo* testing.

4. Materials and methods

4.1. Production of WT-ATR and mutant ATR proteins

The expression plasmid pDEST17 encoding human ATR (NM_001184.3, NP_001175.2) with an N-terminal His_6-tag, but lacking the mitochondrial sequence (Source BioScience, Nottingham, UK), was used to transform *E. coli* BL21StarTMDE3 One Shot Cells (Invitrogen, Carlsbad, CA, USA). ATR mutations were introduced by site-directed mutagenesis using the QuikChange Mutagenesis Kit (Stratagene, Cedar Drive, TX, USA) and specially designed primers. All mutated plasmids were verified by DNA sequencing. For protein expression, bacteria were pre-cultured in Luria-Bertani broth (LB) [47] supplemented with 40 mM glucose, and containing 100 μg/mL ampicillin, overnight at 37 °C. Pre-cultured bacteria were then transferred to a new culture of LB containing 100 μg/mL ampicillin, incubated at 37 °C until an optical density of 0.6, and induced with 0.5 mM IPTG for 5 h. Cells were harvested by centrifugation and lysed by sonication after resuspension in in 50 mM HEPES (pH 7.5), 10 mM Imidazole, 5% glycerol, 0.5 M NaCl, 0.5 mM DTT and 1 × Complete Mini, EDTA-free Protease Inhibitor Cocktail (Roche Applied Biosciences, Indianapolis, IN, US). Insoluble cell debris was removed by centrifugation for 10 min at 5403*g* at 4 °C. Protein concentrations were determined following the Bradford method [48] and using the Bio−Rad Protein Assay Reagent (Bio−Rad Laboratories, Munich, Germany). This crude soluble cell extract was used for protein purification.

Protein purification was performed using the ÄKTA Prime System (GE Healthcare, Little Chalfont, UK) at 4 °C. The crude extract was loaded onto a HisTrap™ High Performance affinity column (GE Healthcare, Little Chalfont, UK) equilibrated with 50 mM HEPES (pH 7.5), 20 mM imidazole, 0.5 M NaCl, 5% glycerol, and eluted with an imidazole gradient from 20 mM to 1 M. The eluted protein fractions were pooled and loaded onto a Superdex 200 HiLoad 16/60 size exclusion chromatography column (GE Healthcare, Little Chalfont, UK). The elution fraction corresponding to trimeric ATR was collected and frozen for further experiments. The pure protein concentration was estimated by measuring the absorbance at 280 nm in a Nanodrop spectrophotometer (Thermo Scientific, Waltham, MA, USA) using the theoretical molar extinction coefficient estimated from the amino acid composition of His_6-ATR (19,160 M^{-1} cm^{-1}). The percentages corresponding to the area of each peak (aggregates, trimers and monomers) were calculated based on their elution time in the size exclusion chromatogram using the Superdex 200 HiLoad 16/60 column and the *Prime View Evaluation* software.

4.2. Differential scanning fluorimetry

The stability of purified wild-type and mutant ATR was assessed by DSF [49], monitoring thermal denaturation in the presence of the extrinsic fluorescent probe SYPRO Orange (Sigma-Aldrich, St. Louis, MO, USA). Final volumes of 50 μL containing 0.05 mg/mL of pure ATR (1.87 μM ATR subunit) in 20 mM HEPES (pH 7.5), 0.5 M NaCl, 5% glycerol, 0.5 mM DTT and 5 × SYPRO Orange were dispensed into LightCycler480 96-well PCR plates (Roche Applied Sciences, Indianapolis, USA). These were then loaded into a Light Cycler 480 (Roche Applied Sciences, Indianapolis, USA) for thermal denaturation. Unfolding curves were recorded from 20 °C to 85 °C at a scan rate of 2 °C/min. The increase in SYPRO Orange fluorescence intensity associated with protein unfolding ($\lambda_{excitation}$ = 465 nm; $\lambda_{emission}$ = 580 nm) was monitored as a measure of thermal denaturation. The midpoint melting temperatures (T_m) were determined as the maximum derivative of the fluorescence curves using in-house software.

The concentration-dependent stabilization of ATR 0.05 mg/mL (1.87 μM ATR subunit) by compounds V and VI was investigated using the same protocol, but with preincubation of ATR with 0–200 μM of each compound prior to denaturation. The K_d for compound VI was calculated from the plot of T_m-values *versus* compound concentration (1–100 μM) by regression analysis using Sigmaplot (Systat Software Inc., San Jose, CA) and the following equation [22]:

$$T_m(L) = \frac{\Delta H_0^* \, T_{m,0}}{\Delta H_0 - n^* R^* T_{m,0}^* \, ln \frac{K_d + L}{K_d}}$$

where ΔH_0 is the enthalpy of unfolding protein-ligand complex, T_m is the midpoint melting temperature at ligand concentration L, $T_{m,0}$ melting temperature without ligand, n is the number of binding sites, R is the gas constant, and K_d is the dissociation constant. The ligand is assumed to bind to the folded protein.

4.3. Western blotting

Samples were subjected to electrophoresis in 10% NuPAGE® Bis-Tris Precast Gels (Invitrogen, Carlsbad, CA, USA). ProSieve® Color Protein Markers (Lonza, Basel, Switzerland) were used as molecular weight markers. Proteins were transferred to a nitrocellulose membrane using the iBlot® Dry Blotting System (Invitrogen, Carlsbad, CA, USA). Membranes were blocked for at least 1 h with 0.1% PBS-Tween and 5% low fat milk. Immunodetection was performed using primary rabbit polyclonal antibody (11137-1-AP; ProteinTech Group, Inc., Chicago, IL,

USA). Conjugated goat-anti rabbit immunoglobulin G (IgG)-horseradish peroxidase (Santa Cruz Biotechnology, Santa Cruz, CA, USA) was used as the secondary antibody. The Enhanced Chemiluminescence System (GE Healthcare, Little Chalfont, UK) was used for detection.

4.4. Cellular model used to assess ATR activity in the absence and presence of the potential PCs

The full-length cDNA of human ATR was cloned into the mammalian lentiviral plasmid pReceiver-Lv158 (EX-T2465-Lv158) which contains the FLAG tag prior to the multiple cloning site (GeneCopoeia, Rockville, MD). ATR mutations (p.Arg186Gln, p.Arg186Trp, p.Arg190Cys, p.Arg190His, p.Arg191Gln and p.Glu193Lys) were introduced by site-directed mutagenesis using the QuikChange Mutagenesis Kit (Stratagene, Cedar Drive, TX, USA) and specially designed primers. The resulting constructs were transduced into a patient-derived fibroblast cell line showing null ATR expression (c.290 G > A/c.349–1 G > C). Lentiviral stock production and fibroblast infection were performed as described elsewhere [50]. Successfully infected fibroblasts were selected by geneticin treatment.

5×10^4 transduced cells were plated and grown at 37 °C for 24 h in MEM medium supplemented with 2 mM glutamine, 10% fetal bovine serum, antibiotics, and 250 μg/mL of geneticin. The previous medium was discarded and cells were then incubated with 80 μM of compound V, and/or 5 μM of compound VI, and/or 1 μg/mL of OHCbl, and 0.2% of DMSO for 72 h in MEM without geneticin. The cells were then incubated at 37 °C for 18 h in the presence of Puck's saline solution containing glucose (0.5 mM), fetal calf serum (15%), propionate (1 mM) and 1 μCi/mL of of [^{14}C]-propionate, harvested by trypsinization followed by centrifugation for 5 min at 15,871*g* and used to determine ATR activity. ATR activity was measured in a coupled assay *via* the incorporation of [^{14}C]-propionate into acid-precipitable proteins as previously described [21]. After centrifugation, TCA-precipitated material was re-suspended in NaOH 0.5 N. Incorporation of [^{14}C]-propionate into trichloroacetic acid (TCA) precipitate was estimated by re-suspending the samples in scintillation liquid and radioactivity quantification was performed in a Wallac RackBeta 1219 liquid scintillation counter (PerkinElmer, Waltham, MA, USA). The data was referred to the corresponding amount of protein, which was measured by the Lowry method.

4.5. Cellular viability assay

Cell viability assays were performed using the CellTiter 96® AQueous One Solution Cell Proliferation Kit (Promega, Madison, Wisconsin, USA) in 96-well plates. Patient-derived fibroblasts showing null ATR expression (c.290 G > A/c.349–1 G > C) were seeded at a density of 15,000 cells per well in MEM supplemented with 1% glutamine, antibiotics and 5% FCS to reduce any possible background interference. HepaRG™ cells (Thermo Fisher Scientific, Grand Island, NY, USA), were seeded at high-density in William's E medium (Gibco, Grand Island, NY, USA) supplemented with glutamax I (Thermo Fisher Scientific, Grand Island, NY, USA), 10% FCS, antibiotics, bovine insulin (5 μg/mL, Sigma-Aldrich, St. Louis, MO, USA) and hydrocortisone 21-hemisuccinate sodium salt (50 μM, Sigma-Aldrich, St. Louis, MO, USA). Medium was then replaced by fresh medium containing one of the two selected potential PCs at different concentrations, and the cells incubated at 37 °C for 72 h. Then, the culture medium was replaced again by fresh medium containing 3-(4,5-dimethyl-2-yl)-5-(3-carboxymethoxyphenyl)-2-(4-sulphophenyl)-2H-tetrazolium, inner salt (MTS) and the cells were incubated at 37 °C for 30 min for colour development. Absorbance was measured at 490 nm using an EL 340 microplate bio-kinetics reader (BioTek Instruments, Winooski, VT, USA). The background absorbance shown at zero cells/well was subtracted from the final data.

Virtual pharmaco-chemical analysis of the hit compounds.

The pharmaco-chemical analysis of the compounds was performed using the SmartsFilter program (http://pasilla.health.unm.edu/tomcat/biocomp/smartsfilter). All analyses were performed under the “normal” and “analyse one molecule” modes. The SMARTS (http://www.daylight.com/dayhtml/doc/theory/theory.smarts.html) sets used were: Glaxo, Blake, ALARM NMR, PAINS and Oprea [23,25,28–30].

4.6. Molecular docking

Potential binding sites for compound VI were identified using an automated molecular-docking procedure in the web-based SwissDock program [51,52], employing the “Accurate” parameter at otherwise default parameters, with no region of interest defined (blind docking).

4.7. Statistics

Data are reported as the mean ± SD. Statistical analyses (one-way ANOVA followed by a Bonferroni *post hoc* test) were performed using IBM SPSS Statistics v.21 software for Windows.

Transparency document

The Transparency document associated with this article can be found, in online version.

Acknowledgements

The authors thank Nooshin Bayat, Jon Gil and Pedro Martínez for helpful contributions.

Funding

This work was supported by *Instituto de Salud Carlos III* and (grant PI13/01239) plus grants from the *Fundación Isabel Gemio and Obra Social de La Caixa* to BP; the Research Council of Norway [nr. 185181 to AM], The KG Jebsen Foundation, and NovoSeeds (Novo Nordisk). AG was supported by a *Ramón y Cajal* grant from the *Ministerio de Ciencia y Tecnología*. This work was supported also by the European Regional Development Fund (PI13/01239).

Conflict of interest statement

None declared.

Appendix A. Supplementary data

Supplementary data to this article can be found online at https://doi.org/10.1016/j.bbadis.2017.11.024.

References

[1] D.S. Froese, R.A. Gravel, Genetic disorders of vitamin B(1)(2) metabolism: eight complementation groups–eight genes, Expert Rev. Mol. Med. 12 (2010) e37.
[2] H.L. Schubert, C.P. Hill, Structure of ATP-bound human ATP:cobalamin adenosyltransferase, Biochemistry 45 (2006) 15188–15196.
[3] B. Merinero, B. Perez, C. Perez-Cerda, A. Rincon, L.R. Desviat, M.A. Martinez, P.R. Sala, M.J. Garcia, L. Aldamiz-Echevarria, J. Campos, V. Cornejo, M. Del Toro, A. Mahfoud, M. Martinez-Pardo, R. Parini, C. Pedron, L. Pena-Quintana, M. Perez, M. Pourfarzam, M. Ugarte, Methylmalonic acidaemia: examination of genotype and biochemical data in 32 patients belonging to mut, cblA or cblB complementation group, J. Inherit. Metab. Dis. 31 (2008) 55–66.
[4] C.M. Dobson, T. Wai, D. Leclerc, H. Kadir, M. Narang, J.P. Lerner-Ellis, T.J. Hudson, D.S. Rosenblatt, R.A. Gravel, Identification of the gene responsible for the cblB complementation group of vitamin B12-dependent methylmalonic aciduria, Hum. Mol. Genet. 11 (2002) 3361–3369.
[5] B. Fowler, J.V. Leonard, M.R. Baumgartner, Causes of and diagnostic approach to methylmalonic acidurias, J. Inherit. Metab. Dis. 31 (2008) 350–360.
[6] A.K. Niemi, I.K. Kim, C.E. Krueger, T.M. Cowan, N. Baugh, R. Farrell, C.A. Bonham, W. Concepcion, C.O. Esquivel, G.M. Enns, Treatment of methylmalonic acidemia by liver or combined liver-kidney transplantation, J. Pediatr. 166 (2015) 1455–1461

(e1451).
[7] A. Jorge-Finnigan, C. Aguado, R. Sanchez-Alcudia, D. Abia, E. Richard, B. Merinero, A. Gamez, R. Banerjee, L.R. Desviat, M. Ugarte, B. Perez, Functional and structural analysis of five mutations identified in methylmalonic aciduria cblB type, Hum. Mutat. 31 (2010) 1033–1042.
[8] A. Jorge-Finnigan, S. Brasil, J. Underhaug, P. Ruiz-Sala, B. Merinero, R. Banerjee, L.R. Desviat, M. Ugarte, A. Martinez, B. Perez, Pharmacological chaperones as a potential therapeutic option in methylmalonic aciduria cblB type, Hum. Mol. Genet. 22 (2013) 3680–3689.
[9] M. Radwan, R.J. Wood, X. Sui, D.M. Hatters, When proteostasis goes bad: protein aggregation in the cell, IUBMB Life 69 (2017) 49–54.
[10] I. Amm, T. Sommer, D.H. Wolf, Protein quality control and elimination of protein waste: the role of the ubiquitin-proteasome system, Biochim. Biophys. Acta 2014 (1843) 182–196.
[11] A.C. Muntau, J. Leandro, M. Staudigl, F. Mayer, S.W. Gersting, Innovative strategies to treat protein misfolding in inborn errors of metabolism: pharmacological chaperones and proteostasis regulators, J. Inherit. Metab. Dis. 37 (2014) 505–523.
[12] W.W. Yue, From structural biology to designing therapy for inborn errors of metabolism, J. Inherit. Metab. Dis. 39 (2016) 489–498.
[13] N.J. Leidenheimer, K.G. Ryder, Pharmacological chaperoning: a primer on mechanism and pharmacology, Pharmacol. Res. 83 (2014) 10–19.
[14] J. Aymami, X. Barril, L. Rodriguez-Pascau, M. Martinell, Pharmacological chaperones for enzyme enhancement therapy in genetic diseases, Pharm. Pat. Anal. 2 (2013) 109–124.
[15] C. Porto, M.C. Ferrara, M. Meli, E. Acampora, V. Avolio, M. Rosa, B. Cobucci-Ponzano, G. Colombo, M. Moracci, G. Andria, G. Parenti, Pharmacological enhancement of alpha-glucosidase by the allosteric chaperone N-acetylcysteine, Mol. Ther. 20 (2012) 2201–2211.
[16] E.K. Jaffe, L. Stith, S.H. Lawrence, M. Andrake, R.L. Dunbrack Jr., A new model for allosteric regulation of phenylalanine hydroxylase: implications for disease and therapeutics, Arch. Biochem. Biophys. 530 (2013) 73–82.
[17] Y.J. Wang, X.J. Di, T.W. Mu, Using pharmacological chaperones to restore proteostasis, Pharmacol. Res. 83 (2014) 3–9.
[18] T.W. Mu, D.S. Ong, Y.J. Wang, W.E. Balch, J.R. Yates 3rd, L. Segatori, J.W. Kelly, Chemical and biological approaches synergize to ameliorate protein-folding diseases, Cell 134 (2008) 769–781.
[19] J. Zhang, C.M. Dobson, X. Wu, J. Lerner-Ellis, D.S. Rosenblatt, R.A. Gravel, Impact of cblB mutations on the function of ATP:cob(I)alamin adenosyltransferase in disorders of vitamin B12 metabolism, Mol. Genet. Metab. 87 (2006) 315–322.
[20] J. Zhang, X. Wu, D. Padovani, H.L. Schubert, R.A. Gravel, Ligand-binding by catalytically inactive mutants of the cblB complementation group defective in human ATP:cob(I)alamin adenosyltransferase, Mol. Genet. Metab. 98 (2009) 278–284.
[21] C. Perez-Cerda, B. Merinero, P. Sanz, A. Jimenez, M.J. Garcia, A. Urbon, J. Diaz Recasens, C. Ramos, C. Ayuso, M. Ugarte, Successful first trimester diagnosis in a pregnancy at risk for propionic acidaemia, J. Inherit. Metab. Dis. 12 (Suppl. 2) (1989) 274–276.
[22] A. Cooper, K. McAuley-Hecht, Microcalorimetry and the molecular recognition of peptides and proteins, Philos. Trans. R. Soc. Lond. 345 (1993) 23–35.
[23] J.B. Baell, G.A. Holloway, New substructure filters for removal of pan assay interference compounds (PAINS) from screening libraries and for their exclusion in bioassays, J. Med. Chem. 53 (2010) 2719–2740.
[24] T. Tomasic, L. Peterlin Masic, Rhodanine as a scaffold in drug discovery: a critical review of its biological activities and mechanisms of target modulation, Expert Opin. Drug Discovery 7 (2012) 549–560.
[25] J.R. Huth, R. Mendoza, E.T. Olejniczak, R.W. Johnson, D.A. Cothron, Y. Liu, C.G. Lerner, J. Chen, P.J. Hajduk, ALARM NMR: a rapid and robust experimental method to detect reactive false positives in biochemical screens, J. Am. Chem. Soc. 127 (2005) 217–224.
[26] D.F. Veber, S.R. Johnson, H.Y. Cheng, B.R. Smith, K.W. Ward, K.D. Kopple, Molecular properties that influence the oral bioavailability of drug candidates, J. Med. Chem. 45 (2002) 2615–2623.
[27] P. Ertl, B. Rohde, P. Selzer, Fast calculation of molecular polar surface area as a sum of fragment-based contributions and its application to the prediction of drug transport properties, J. Med. Chem. 43 (2000) 3714–3717.
[28] J.F. Blake, Identification and evaluation of molecular properties related to preclinical optimization and clinical fate, Med. Chem. 1 (2005) 649–655.
[29] M. Hann, B. Hudson, X. Lewell, R. Lifely, L. Miller, N. Ramsden, Strategic pooling of compounds for high-throughput screening, J. Chem. Inf. Comput. Sci. 39 (1999) 897–902.
[30] T.I. Oprea, I. Zamora, A.L. Ungell, Pharmacokinetically based mapping device for chemical space navigation, J. Comb. Chem. 4 (2002) 258–266.
[31] M. Wastfelt, B. Fadeel, J.I. Henter, A journey of hope: lessons learned from studies on rare diseases and orphan drugs, J. Intern. Med. 260 (2006) 1–10.
[32] P. Yuste-Checa, S. Brasil, A. Gamez, J. Underhaug, L.R. Desviat, M. Ugarte, C. Perez-Cerda, A. Martinez, B. Perez, Pharmacological chaperoning: a potential treatment for PMM2-CDG, Hum. Mutat. 38 (2017) 160–168.
[33] J.P. Lerner-Ellis, A.B. Gradinger, D. Watkins, J.C. Tirone, A. Villeneuve, C.M. Dobson, A. Montpetit, P. Lepage, R.A. Gravel, D.S. Rosenblatt, Mutation and biochemical analysis of patients belonging to the cblB complementation class of vitamin B12-dependent methylmalonic aciduria, Mol. Genet. Metab. 87 (2006) 219–225.
[34] G. Parenti, Treating lysosomal storage diseases with pharmacological chaperones: from concept to clinics, EMBO Mol. Med. 1 (2009) 268–279.
[35] C. Porto, M. Cardone, F. Fontana, B. Rossi, M.R. Tuzzi, A. Tarallo, M.V. Barone, G. Andria, G. Parenti, The pharmacological chaperone N-butyldeoxynojirimycin enhances enzyme replacement therapy in Pompe disease fibroblasts, Mol. Ther. 17 (2009) 964–971.
[36] K.J. Valenzano, R. Khanna, A.C. Powe, R. Boyd, G. Lee, J.J. Flanagan, E.R. Benjamin, Identification and characterization of pharmacological chaperones to correct enzyme deficiencies in lysosomal storage disorders, Assay Drug Dev. Technol. 9 (2011) 213–235.
[37] J.W. Hanrahan, H.M. Sampson, D.Y. Thomas, Novel pharmacological strategies to treat cystic fibrosis, Trends Pharmacol. Sci. 34 (2013) 119–125.
[38] J. Macias-Vidal, M. Giros, M. Guerrero, P. Gascon, J. Serratosa, O. Bachs, M.J. Coll, The proteasome inhibitor bortezomib reduced cholesterol accumulation in fibroblasts from Niemann-pick type C patients carrying missense mutations, FEBS J. 281 (2014) 4450–4466.
[39] A.L. Pey, M. Ying, N. Cremades, A. Velazquez-Campoy, T. Scherer, B. Thony, J. Sancho, A. Martinez, Identification of pharmacological chaperones as potential therapeutic agents to treat phenylketonuria, J. Clin. Invest. 118 (2008) 2858–2867.
[40] S. Santos-Sierra, J. Kirchmair, A.M. Perna, D. Reiss, K. Kemter, W. Roschinger, H. Glossmann, S.W. Gersting, A.C. Muntau, G. Wolber, F.B. Lagler, Novel pharmacological chaperones that correct phenylketonuria in mice, Hum. Mol. Genet. 21 (2012) 1877–1887.
[41] A. Whitty, Growing PAINS in academic drug discovery, Future Med. Chem. 3 (2011) 797–801.
[42] J.L. Dahlin, J. Inglese, M.A. Walters, Mitigating risk in academic preclinical drug discovery, Nat. Rev. Drug Discov. 14 (2015) 279–294.
[43] J.B. Baell, Screening-based translation of public research encounters painful problems, ACS Med. Chem. Lett. 6 (2015) 229–234.
[44] C.A. Lipinski, F. Lombardo, B.W. Dominy, P.J. Feeney, Experimental and computational approaches to estimate solubility and permeability in drug discovery and development settings, Adv. Drug Deliv. Rev. 46 (2001) 3–26.
[45] C.A. Lipinski, Lead- and drug-like compounds: the rule-of-five revolution, Drug Discov. Today Technol. 1 (2004) 337–341.
[46] K. Zakikhan, B. Pournasr, M. Vosough, M. Nassiri-Asl, In vitro generated hepatocyte-like cells: a novel tool in regenerative medicine and drug discovery, Cell J. 19 (2017) 204–217.
[47] G. Bertani, Studies on lysogenesis. I. The mode of phage liberation by lysogenic *Escherichia coli*, J. Bacteriol. 62 (1951) 293–300.
[48] M.M. Bradford, A rapid and sensitive method for the quantitation of microgram quantities of protein utilizing the principle of protein-dye binding, Anal. Biochem. 72 (1976) 248–254.
[49] F.H. Niesen, H. Berglund, M. Vedadi, The use of differential scanning fluorimetry to detect ligand interactions that promote protein stability, Nat. Protoc. 2 (2007) 2212–2221.
[50] E. Richard, L.R. Desviat, M. Ugarte, B. Perez, Oxidative stress and apoptosis in homocystinuria patients with genetic remethylation defects, J. Cell. Biochem. 114 (2013) 183–191.
[51] L. Bonello, N. Bonello, C. Grosdidier, L. Camoin-Jau, Unveiling the mysteries of clopidogrel metabolism and efficacy, Clin. Pharmacol. Ther. 90 (2011) 774–776.
[52] A. Grosdidier, V. Zoete, O. Michielin, Fast docking using the CHARMM force field with EADock DSS, J. Comput. Chem. 32 (2011) 2149–2159.